SEISMIC PERFORMANCE OF DAMAGE-PROTECTED BEAM-COLUMN JOINTS

Journal:	*ACI Structural and Materials Journals*
Manuscript ID:	S-2006-467
Journal Name:	ACI Structural Journal
Date Submitted by the Author:	01-Dec-2006
Complete List of Authors:	Solberg, Kevin; University of Canterbury NZ; Univ of Canterbury, Civil Engineering Dhakal, Rajesh; University of Canterbury NZ Mander, John; Univ of Canterbury, Civil Engineering Li, Luoman; University of Canterbury NZ Bradley, Brendon; Univ of Canterbury, Civil Engineering
Keywords:	Damage Avoidance Design (DAD), Quasi-Earthquake Displacement (QED) test, Multi-level Seismic Performance Assessment (MSPA)

SEISMIC PERFORMANCE OF DAMAGE-PROTECTED BEAM-COLUMN JOINTS

Kevin Solberg, Rajesh P Dhakal, John B Mander, Luoman Li and Brendon Bradley

Biography: ACI member **Rajesh P Dhakal** is a Senior Lecturer in the Civil Engineering Department at University of Canterbury. He received his BS from Tribhuvan University, ME from AIT and PhD from the University of Tokyo. His research interests include performance based earthquake engineering and analytical modeling of structural behaviors.

ACI member **John B Mander** is a Chair Professor in the Civil Engineering Department at University of Canterbury. He received his BS and PhD from University of Canterbury. His research interests include performance evaluation of structures through experimental investigation and damage avoidance design of structures.

Kevin Solberg, Luoman Li and Brendon Bradley are graduate students in the Civil Engineering Department at University of Canterbury.

ABSTRACT

An experimental and computational study of an 80 percent scale precast concrete 3D beam-column joint sub-assembly designed with damage protected rocking connections is presented. A prestress system is implemented whereby high-alloy high-strength unbonded thread-bars running through the beams are coupled to rods within the columns. The thread-bars are post-tensioned and supplemental energy dissipation devices are also installed. Both wet and dry joint solutions are considered. A *Multi-level Seismic Performance Assessment* (MSPA) is conducted considering three performance objectives related to occupancy and collapse prevention. First, bi-directional quasi-static cyclic tests are conducted and the specimen's

performance characterized. This data is then used in a 3D nonlinear *Incremental Dynamic Analysis* (IDA). Results from the IDA are used to select three critical earthquakes for further experimental bi-directional testing. Thus quasi-earthquake displacement tests are performed. Results indicate the system satisfies all performance objectives related to serviceability and life-safety. Further design improvements are discussed.

Keywords: Damage Avoidance Design (DAD); Quasi-Earthquake Displacement (QED) test; Multi-level Seismic Performance Assessment (MSPA).

INTRODUCTION

Current seismic design accepts that damage will occur in moderate to large seismic events, although attempts are made via special detailing to limit this damage to specific plastic hinge zones. These zones, designed to sustain severe damage under multiple cyclic rotations, tend to act like a fuse, essentially protecting the structure from forming unfavorable mechanisms. Although this design philosophy ensures good protection to occupants by preventing collapse, there is a strong likelihood a moderate to large earthquake will render a structure irreparable. As a result, economic costs, both direct and indirect, can be significant; this has been confirmed from recent earthquakes in the United States (Northridge, 1994) and Japan (Kobe, 1995). To address this issue, alternative structural systems have been proposed where precast concrete elements are designed to remain essentially elastic, with inelastic behavior accommodated for by rocking at specially detailed joints.

The theoretical basis of rocking systems has been investigated by many early researchers[1, 2]. Although it was not until more recently[3] that so-called "hybrid" systems were introduced. These systems utilize full or partially unbonded post-tensioned prestress to provide a restoring force and supplemental yielding devices to provide energy dissipation. By

combining the hysteretic behavior of these two components, it is possible for a joint to exhibit a combination of bi-linear elastic (post-tensioning) and elasto-plastic (yielding devices) hysteresis behavior. The result is a flag shaped hysteresis loop, displaying good energy dissipation and re-centering characteristics.

As part of a large research project in the United States, the PRESSS program investigated the behavior of these systems through testing of many sub-assemblages[3] and a five-storey 3D frame and wall system[4]. The system performed well with much less damage than would be expected with monolithic construction. Little residual displacement was observed in both frames and walls. The details used however, employed a concrete-concrete or high-strength grout interface, resulting in some damage at the joint region.

Mander and Cheng[5] proposed a new seismic design and construction philosophy for bridges called *Damage Avoidance Design* (DAD). In this approach, joints are armored with steel to protect them from damage incurred from rocking. This concept was validated by bi-directional tests performed on a scaled bridge pier[6]. Results indicate little damage at the joint and good bi-linear elastic behavior. More recently, these concepts have been further developed in New Zealand and design guidelines for such ductile jointed precast concrete systems have been introduced into the concrete code[7] as an appendix. The aim of such a system is to allow for rapid on-site erection, thereby reducing initial costs. As part of an ongoing research program at the University of Canterbury, further experimental investigations have been conducted[8-11] with the goal of refining detailing at the joint and providing cost-effective alternative solutions. As a follow up to this previous work, this paper presents results from a combined experimental and computational study on the bi-directional behavior of DAD beam-column joints.

RESEARCH SIGNIFICANCE

Two research objectives will be addressed herein. Firstly, previous research adopted quasi-static testing, in which loading was composed of regulated displacement cycles. These cycles however, are not completely representative of the displacement demands due to seismic excitation. Therefore, this study will adopt the *Quasi-Earthquake Displacement* (QED)[12] test method, where the specimen will be subjected to displacement profiles found analytically using real ground motion records. Using this approach, a *Multi-level Seismic Performance Assessment* (MSPA)[13] will be conducted, characterizing the performance of the specimen at multiple levels of seismic demand. Secondly, further refinement of the beam-column joint details is needed to ensure a practical, cost-effective solution. Li[10] investigated the behavior of a beam-column joint using a bent coupler system whereby high-strength thread-bars in a beam are coupled to diagonal rods running through the column. The aim of such a system is to allow for rapid on-site erection, thereby reducing initial costs. From physical testing, it was found that its performance was satisfactory; however several design improvements relating to the coupler system and the armored ends were suggested. This study implements these design improvements and ensures the provided detailing satisfies performance objectives relating to immediate occupancy and collapse prevention.

EXPERIMENTAL INVESTIGATION

Prototype structure

As shown in **Fig. 1**, the prototype is a ten-storey reinforced concrete frame building with three 10m bays in each direction. This generic structure, commonly known as the "red book" building[14], was designed according to the New Zealand concrete standard[7] for intermediate soil in Christchurch, New Zealand. Keeping all other variables constant, the same structure was designed and detailed according to damage avoidance principles, thereby resulting in

precast beams and columns being connected via a post-tensioning system with other devices to provide supplemental energy dissipation. The DAD building was designed with precast flooring units running in the transverse direction and seated on the transverse beams, leaving the longitudinal beams to resist predominately seismic forces.

To help ensure jointed precast systems are adopted by the construction industry , the system must be relatively simple to erect. A major component of this is the post-tensioning system. This study investigates the use of a coupled high strength threaded rods to provide post-tensioning. In this design, it is possible for complete beam and column sections to be cast off-site with rods already in place within the respective elements. Once on-site, the beam's rods are connected via a coupler system to a short rod in the column and anchored to the column's opposite face. A detailed explanation of this and other design elements follows.

Specimen

An exterior joint on the second floor of the prototype structure was taken for the 3D beam-column subassembly. Using constant stress and strain similitude principles, the specimen was scaled to 80%, and consisted of two beams in the longitudinal direction, and one beam in the transverse direction. Herein, the longitudinal and transverse beams are dominated by seismic load and gravity loads (carrying the one-way precast panels) and respectively are referred to as the east-west seismic and north-south gravity beams.

Reinforcing details of the column are given in **Fig. 2**. An axial load of 2000kN due to self weight of the above floors was simulated in the 700x700 mm column by prestressed (Macalloy^{TM}) 32mm diameter high strength threaded rods. Three 20mm thick mild steel plates were cast at the column faces where precast beams were joined. The minimum reinforcement ratio, $\rho_l = 0.008$ was provided using 12 HD20 (f_y = 500MPa) threaded bars (Reidbars^{TM}). This low reinforcement ratio eased congestion in the joint region. To transfer

shear forces through the joint, five double HR12 hoops spaced at 100mm centers were provided. The design compression strength of the column was taken to be f'_c= 45MPa. PVC ducts were placed at a 20 degree angle in each seismic beam and horizontal through the gravity beam for the post-tensioning rods.

Reinforcing details of the seismic beams and gravity beam are given in **Fig. 2** (a) and (b), respectively. A cracked elastic design was used to detail longitudinal reinforcement in the precast beam segments. In this design approach, sufficient quantities of mild steel are provided to ensure that yield of longitudinal reinforcing is prevented and concrete compressive stresses are below $0.7f'_c$. This ensures precast elements remain essentially elastic even when the connection reaches over-strength. Shear design of the precast elements followed the New Zealand concrete code[7] with a total initial axial load of 400kN provided by the post-tensioning rods. Within the mid section of the beams, only minimal transverse steel was used, thus a stirrup spacing of *d/2* was adopted. A tighter, 100mm spacing was provided at the ends. Additional stirrups near the joint were provided to provide confinement for the concrete to withstand large compressive stress expected in the end regions.

All beams were 560mm deep by 400mm wide. Unbonded post-tensioning was provided by two 26.5mm diameter high strength threaded rods placed in 50mm PVC ducts. The seismic and gravity beams implemented two separate detailing strategies as given below. The gravity beam was detailed according to Li[10]. Instead of a straight coupler, a bent coupler was used for one of the rods. This was done to accommodate a draped profile in the beam. As in the seismic beams, the shorter bolt bar section was machined to 75% of its effective area. A 100x100x12 steel angle was used, with the flange flush against the column face. This required the beam's longitudinal steel to be developed by plug welding it to the back edge of the angle's flange.

A detail of the seismic beam-column joint is given in **Fig. 3**. The seismic beams utilized a straight coupler system where the tendons were pre-bent at the joint end to a radius of approximately 1.8m. This allowed proper alignment with the angled rod running through the column. This shorter rod, termed the 'bolt bar', was machined to 75% of its effective area to ensure any yielding in the post-tensioning system would be limited to the replaceable column bolt bar. At the beam end, a 100x100x12 inverted steel angle was used at top and bottom of the joint, and the face of concrete was recessed 5mm. This ensured that contact with the column was limited to the steel and allowed the angle's buried flange to mechanically develop the beam's longitudinal steel using Reidbar^{TM} nuts.

By the nature of precast concrete and rocking connections, it is critical that the face of the beam be aligned flush with the column. Therefore, offsite erection of a full length beam section may lead to on-site misalignment issues which may affect rocking behaviour. To mitigate this and allow for construction tolerances similar to current standards, a 310mm cast in-situ closure pour was provided on the west seismic beam. This closure pour is implemented on-site after the armouring angles have been adjusted to ensure a flush face at both ends and the post tensioning rods are coupled together. High strength, fibre-reinforced concrete was used in the in-situ end to compare its behaviour to the regular strength concrete of the east beam. The compressive strength of the high strength concrete was tested and found to be f'_c= 70MPa. The east beam and the remainder of the west beam concrete was found to be f'_c= 37MPa.

At each joint, four 30mm diameter shear keys were installed, tapered 5° inward to ensure they do not jam when the specimen rocks. These were designed to be screwed into the face of the column via a cast in double nut. The shear keys were designed for gravity and seismic shear forces. One shear key was located in each corner, providing resistance to torsion.

Supplemental energy dissipation

Supplemental energy dissipation was provided by mild steel bars designed to yield as the specimen rocks at its joints. To facilitate easy replacement, these devices were mounted externally. For the seismic beams, the dissipaters were located at centreline of the beam and anchored to a 32mm thick steel plate set back 300mm from the face of column. The dissipaters ran through a duct in the column and were bolted at each end of the anchor plate and column face, ensuring the devices worked independently at each joint. For the seismic beam, dissipaters were located at top and bottom of the beam, anchored to the beam by a 32mm plate and screwed into nuts cast in the column.

To guarantee the post-tensioning fuse rods are capable of re-centring the system, the energy dissipation devices were designed not to exceed the critical moment capacity of the rods. Note that the post-tensioning rods do not cross the joint at centreline, but rather at the 1/3 point. This meant the dissipaters had to be designed for the minimum eccentricity of the rods, 1/3 the beam depth. The seismic beam dissipaters were machined to a 15mm diameter over a 150mm length and the gravity beam dissipaters were machined to a 12mm diameter over a 200mm length. The devices were designed to buckle when subject to large inelastic cyclic strain.

THEORETICAL BEHAVIOR

Two methods have been introduced for predicting the behavior of rocking systems. Pampanin et al.[14] proposed using a monolithic beam analogy approach. An iterative process is used to determine the neutral axis depth and strain in the compression concrete. Although it has been demonstrated this method agrees well with experimental results, it was developed for precast members without armoring. If armoring is considered, such an analogy is difficult

to conceptualize since the steel develops the compressive forces in a different manner than a typical monolithic beam. As investigated by Mander and Cheng[5] and Li[10], the theoretical behavior of an armored rocking system can best be determined from coupling elastic deformation with rigid body kinematics. In this method, the post-joint opening neutral axis is assumed to be negligible, thus allowing one to presume the specimen rocks on an extreme edge. Using this approach, it is possible to calculate the moment capacity and stiffness at several key response milestones, namely the initiation of gap-opening, yielding of the steel energy dissipaters, and yielding of the post-tensioning tendons. The moment capacity of the joint is calculated by the summation of the contribution from post-tensioning and dissipation devices:

$$M = \sum M_{PS} + \sum M_{diss} \quad (1)$$

given that

$$M_{PS}^{\pm} = P_{PS} e_{PS}\,;\; M_{diss}^{\pm} = P_{diss} e_{diss} \quad (2)$$

where e is the vertical distance of the tendon or dissipaters from the rocking edge of the beam section and P is the force in the prestressed tendon (denoted as P_{PS}) or in the dissipater (denoted as P_{diss}). Since the tendons at the joint were offset from centerline, $e_{PS}^{+} = 187$mm and $e_{PS}^{-} = 373$mm. The energy dissipation devices were at centerline, therefore, $e_{diss}^{+} = e_{diss}^{-} = 280$mm. The force in the tendons can be calculated as:

$$P_{PS} = P_i + \frac{A_{PS} E_{PS}}{L_t} e_{PS} \theta_{con} n \quad (3)$$

where P_i = initial post-tensioning force (200kN); E_{PS} = elastic modulus of the tendon (170,000MPa); A_{PS} = cross sectional area of the tendon (552mm^2); L_t = unbonded length of the tendon (5.25m); θ_{con} = connection rotation; and n = number of joint openings spanned by the tendon (taken as 1 in this case for both directions). The force from the steel dissipaters was simply taken as the yield strength of the devices (60kN per device), and for a device on

each side the combined total force was 120kN. For simplicity strain hardening of these devices was not considered.

The theoretical moment-rotation response of a typical rocking connection is given in **Fig. 4 (a)**. The initial clamping force from P_i is used to calculate the moment capacity at gap-opening, M_{pt}, using Equation (2). This is illustrated by the thin dashed line in the figure. When the dissipation devices are considered, their contribution can be included in the calculation as shown in the figure. The yield elongation of the dissipation devices can be shown to be very small. In this case, the length of the devices in the EW direction is 150mm. Given a yield strain of 0.0015, this equates to a rotation of 0.0008 given the beam depth and dissipater eccentricity in the specimen. This rotation is small enough to be neglected and the devices can be assumed to yield upon gap-opening. Upon unloading, the dampers will be forced into compression. The unloading moment capacity can now be calculated by taking the negative moment contribution of the dissipation devices, as shown by the unloading line of **Fig. 4 (b)**. Finally, the rotation at which the thread-bars yield is found by back calculating given the yield strain of the thread-bars using Equation (3).

The moment capacity of the joint can be related to the lateral force V_{col} by:

$$V_{col} = 2M \frac{L}{L_b L_c} \tag{4}$$

where L = centerline length of the beam (9.8m); L_b = clear support length of the beam (9.1m); and L_c = storey height (2.8m).

The total top displacement of the system given V_{col} can be attributed to localized rotation at the joint and the total elastic deformation of the system:

$$\Delta = \Delta_{elastic} + \theta_{joint} \frac{L_b}{L} L_c \tag{5}$$

where θ_{joint} = joint rotation angle and $\Delta_{elastic}$ is the elastic deformation of the system from flexure, which is limited by the maximum lateral force at uplift. This is derived using the moment area theorem as:

$$\Delta_{elastic} = \frac{V_{col,uplift}}{12}\left[\frac{(L_c - D)^3}{EI^*_{col}} + \frac{L_c^{\,2} L_b^{\,3}}{L^2 EI^*_{bm}}\right] \quad (6)$$

where EI^*_{bm} and EI^*_{col} are the effective stiffness of the beam and column, respectively, and D is the depth of the beams (580mm). An effective stiffness of $0.25I_{gross}$ was used for the beam, as recommended by Li[10]. Based on these equations, the theoretical pushover curve for the subassembly in the EW direction is given in **Fig. 4 (b)** up to a joint rotation of 0.02 radians. The thin dashed line indicates the theoretical force-displacement response from prestress alone.

TEST SETUP AND METHODS

Fig. 5 presents a plan view and two elevations of the test setup. Loads were applied to the specimen by three hydraulic actuators. Actuators A and B were installed to the reaction frame and top of the west and south face of the column, respectively. Actuator C (shown in **Fig. 5 (a)**) was installed in the East-West direction at the end of the gravity beam. This actuator was intended to keep the specimen movement in-plane during uni-directional testing and provide a measure of torsion in the specimen. Actuator C's movement was synchronized to approximately one half the displacement of Actuator A. A constant 120kN load was applied at midsection of the gravity beam through a 300kN hydraulic jack, simulating the weight of the precast flooring panels. The load was spread over a 1.5m timber block and developed into the strong floor through four high strength threaded rods. Load cells were installed in series with each actuator. Additional load cells were attached at the strut of each

beam and the jacking point of each post-tensioned rod. A photograph of the specimen is shown in **Fig. 5 (c)**.

To measure rotation at the joint, 3 linear potentiometers were installed on both faces of each joint, totaling 18 devices. Two additional linear potentiometers were installed against the bottom face of each beam to measure vertical movement. At 8 locations around the specimen (see **Fig. 5 (b)**) rotary potentiometers were installed to measure local displacement. Two 5mm strain gauges were installed on each bolt bar to measure any potential yielding that may occur during testing.

Due to the unique nature of a structural system designed to avoid damage, it was possible to conduct a wide range of tests on the specimen. These included uni-directional and bi-directional quasi-static tests, where the structure was deformed to controlled cyclic loading patterns, and QED tests, where more realistic loading patterns were adopted. The latter method is similar to a pseudodynamic test in that the structure is displaced through 'real' seismic displacements. In QED testing, an inelastic analytical model of the prototype structure is created and subject to an earthquake record of interest. Displacement of the node representing the physical specimen is extracted and used as the displacement profile for physical testing.

Earthquake identification for MSPA

A 3D analytical model of the prototype structure was developed using Ruaumoko3D[16], an inelastic dynamic analysis program. Development of this model was part of a parallel study conducted by the authors; details can be found elsewhere[17]. The hysteresis properties of the joint were calibrated based on uni-directional physical testing of the specimen. **Fig. 6** gives a comparison between the physical and analytical model up to an inter-story drift of 2%.

In the case of MSPA, it is necessary to select earthquake records that represent the desired level of ground excitation. Following current trends, three performance levels were considered. These levels correspond to an upper bound *design basis earthquake* (DBE), which has a 10% probability of occurrence in 50 years, and a median and upper bound *maximum considered event* (MCE), which has a 2% probability of occurrence in 50 years. Current seismological studies predict *peak ground acceleration* (PGA) at various return periods. However, it is not correct to simply apply any earthquake record that conforms to this definition, as structural response is dependent on a multitude of factors. Therefore, it is necessary to extract earthquake records from a suite of likely candidates that will result in the most severe structural behavior. Such a method has been proposed by Dhakal et al.[13] whereby *Incremental Dynamic Analysis* (IDA)[18] is used to probabilistically determine earthquake records representing multiple performance objectives. This method has been adopted herein and is illustrated in **Fig. 7**. Once an IDA has been conducted earthquake records representing different percentile response at a given *intensity measure* (IM) can be extracted. In this study, records were chosen to yield responses that have non-exceedance probabilities of respectively 90% at DBE, 50% at MCE, and 90% at MCE from a suite of 40 records consisting of medium and near-source ground motions. The selected records are given in **Table 1**.

Performance objectives must be defined for the MSPA. The first performance level relates to immediate occupancy (high confidence) and states that a structure should not need to be repaired after a frequent earthquake. It can be interpreted as: (i) the structure should not incur any damage needing repair when subjected to a DBE with a high non-exceedance probability (taken as 90% in this study). The second and third levels of seismic performance relate to structural reparability (moderate confidence) and collapse prevention (high confidence) at rare earthquakes. These can be interpreted as: (ii) the structure should not be damaged

irreparably when subjected to an MCE with a moderate non-exceedance probability (taken as 50% in this study); and (iii) the structure should not collapse when subjected to an MCE with a high non-exceedance probability. Given these objectives, the DAD specimen will be monitored to ensure these objectives are met, if not exceeded.

RESULTS

Due to space limitations, results are presented only for a bi-directional quasi-static test to 2% drift and the QED tests using the earthquakes selected for MSPA. In all tests, each post-tensioned rod was stressed to 50% of its yield limit (i.e. 200kN). This provided a total of 400kN of post-tensioning force at each joint. The energy dissipaters were replaced after each test.

Quasi-static test results

Fig. 8 presents results of bi-directional test to the design level drift of 2%. The results shown are for a bi-directional "clover leaf" test, where total drift is calculated considering both X and Y components. Note that the individual plots are projected to one another, allowing an easy comparison to be made between the NS and EW direction.

During stressing of the rods, a 1mm crack formed at the bottom edge of each beam, running between the edges of each flange. This crack can be attributed to the vertical component of the diagonal tendons, approximately a 120kN upward force at the joint. This force in effect pulled the beam up the face of the column. The bottom steel flange however, resisted this due to high friction forces, causing tearing just above the angle, as evidenced by this crack.

Opening of the gap was observed at approximately 0.5% drift, at which point the steel dissipaters yielded in tension almost immediately (as evidenced from strain gauges). In the east beam, two hairline cracks formed just before reaching the target drift of 2%, propagating

100mm out from the dissipater anchor plate. The west beam (high-strength concrete) did not suffer additional cracking. Due to the bi-directional rocking, localized crushing was observed behind the top angle of the east beam over a 10mm square area at the top concrete face. At approximately 1% drift, slight buckling of the steel dissipaters occurred as the gap began to close. This was more severe for the gravity beams than the seismic beams, attributed to their longer length. Throughout testing, no damage was observed on the column. A photograph of the east beam after testing is given in **Fig. 9**.

As expected, the seismic beam exhibited bi-linear elastic hysteretic behavior, with some energy dissipation, resulting in a flag-shaped response. Some residual displacement was observed, though this can be partially traced to movement of approximately 2mm in the column base pin, which was repaired for the remaining tests. The unsymmetrical hysteretic response of the gravity beam can be attributed to the inclusion of gravity load, causing an initial positive bending moment at the joint. The gravity beam did not fully re-centre upon removal of the lateral load, resulting in a residual drift of approximately 0.5%. This may be partially attributed to sliding of the base pin.

Quasi-earthquake displacement (QED) test results

Fig. 10 presents results for the seismic beams from the three QED tests. Since the gravity beam had been previously tested as part of a prior study, its response is omitted and can be found elsewhere[10]. Note that these tests were performed after the initial quasi-static tests (up to 2% drift), and therefore some damage to the specimen had already been observed. Nevertheless, these tests will give a more accurate assessment of response from 'real' loading patterns and any additional damage can be attributed to the given demand.

The 90th percentile DBE test consisted of an initial pulse (attributed to the near source record) to the maximum drift of 2.1%. Gap opening and yielding of the energy dissipaters occurred

at around the same drift as in previous testing (~0.5%). No new cracks or additional crushing was observed on the seismic beams. A flag shaped hysteresis loop was observed during the initial pulse; however for the remainder of the test response was mostly elastic. Some post-gap opening stiffness degradation was observed, likely due to yielding and buckling of the energy dissipaters. The maximum gap opening, recorded from the potentiometers was approximately 5mm.

The 50th percentile MCE maximum drift was 2.8%, which, like the previous test, occurred in the first major loading cycle. This resulted in considerable yielding of the dissipaters and buckling upon unloading. Consequently, further cycles exhibited a lower capacity, resulting in strength degradation of approximately 20% on the second cycle. A hairline diagonal crack approximately 300mm long was observed on the east and west beam, appearing to be the result of a compression strut. Small (<100mm) hairline cracks formed along the corners of the steel angles of the east beam; but these cracks closed after the test. As observed from the strain gauges, the bolt bars reached a maximum of 6000 μstrain ($\varepsilon_{yield} \sim 5500$), resulting in slight yielding and an average loss of post-tensioning force of 5%.

The final test, the 90th percentile MCE was the most severe of all tests performed. The maximum drift was 4.7%. Additional crushing was observed along the top and bottom flange of the east beam's steel angle. This crushing was limited to an area of approximately 25mm measured from the flange edge. The bottom flange of the west beam suffered similar crushing, at one end, covering an area of approximately 10mm square. Some spalling was observed over a 25mm area along the angles of both beams. The diagonal cracks formed in previous test approximately doubled in length and opened to about 1.5mm in the east beam, and 0.5mm in the west beam. At the end of testing, these cracks closed. As seen in the figure, a flag-shaped hysteresis loop was observed, with a maximum residual drift of about 0.1%.

The initial (pre-gap opening) stiffness of the specimen remained virtually unchanged, however. Some minor stiffness and strength degradation was observed in the post-gap opening range. The bolt bars reached a maximum strain of 9000 μstrain and maximum force of 360kN, more than the yield capacity of the fuse bar. This resulted in a loss of post-tensioning force of approximately 35%, which is the major cause of observed strength degradation. Since the yield force of the regular 26.5mm tendon is about 400kN, the bolt bar 'fuse' protected the beam rods from yielding. Two photographs of the specimen during this test are given in **Fig. 11**.

Fig. 12 presents a sample comparison of the experimental data and the prediction outlined earlier. The experimental data is for the 50th percentile MCE test. From this comparison it appears the prediction provides reasonable agreement with the experimental data. The transition between pre- and post-rocking is smooth for the physical specimen. Experimentally, the initial stiffness appears to vary slightly, but the prediction does seem to capture the average stiffness. The energy dissipation is marginally more than expected; this is attributed to additional frictional losses within the prestress system itself that arise from relative movements in the vicinity of the bent tendon.

MULTI-LEVEL SEICMIC PERFORMANCE ASSESSMENT (MSPA)

Test results suggest the specimen satisfied all performance objectives relating to occupancy and collapse prevention. By performing QED tests, whereby the specimen is displaced to patterns similar to those expected from real earthquakes, it is possible to provide some insight as to the damage outcomes of such a structure following seismic events.

Considering the first case of immediate occupancy, it was stated that the structure must remain operational following a design level earthquake. This case was represented by a 90th percentile DBE, with a peak drift of 2.1%. Aside from some aesthetic cracks, the structure

did not sustain any damage that affected its response. Yielding of the energy dissipation devices occurred and therefore these would have to be replaced, which may not be a time-consuming job. Hence, it is safe to conclude the structure is likely to remain operational immediately after the frequent earthquakes.

The second objective, ensuring with moderate confidence the structure can be repaired following an 'extreme' seismic event, was verified by the 50th percentile MCE. The maximum drift level for this test was 2.8%, at which point the dissipaters had buckled and slight yielding of the post-tensioning bolt bars had occurred. Since the structure lost some of its stiffness (as provided by the post-tensioning) it would be prudent to close the structure until crews could re-tension the rods and replace the dissipaters. The relative cost of these repairs would be low, since the jack points for the rods and the energy dissipaters are readily accessible.

The third and most important objective, ensuring with a high level of confidence that the structure will not collapse from an 'extreme' earthquake, was verified by a 90th percentile MCE. In this case, the structure was subject to an earthquake demanding a drift of 4.7%. The post-tensioning system suffered considerable yielding (and loss of pre-stress) and the energy dissipaters were severely damaged. However, the specimen remained stable, and even after this extreme drift level, exhibited reasonable hysteretic behavior. In this case, the energy dissipaters would need to be replaced and the post-tensioning system would need to be stressed back up to initial conditions. Since the bolt bars underwent considerable strain, it may be prudent to replace them. The integrity of the concrete, particularly for the high-strength cast in-situ concrete joint, remained high.

DISCUSSION

Overall, the specimen met the requirements outlined in the MSPA. Compared to traditional monolithic construction, the system performed exceptionally well. The most notable advantage of the DAD system was the significantly lower expected repair costs following the 90th percentile MCE. At 4.7% drift, a monolithic beam-column joint would likely experience severe cracking, spalling, and potentially even buckling of longitudinal steel. This would result in significant repair costs of each joint or complete replacement of the structure. Conversely, the DAD system would need its prestressing bars re-tensioned and its energy dissipaters replaced. This would result in at a much lower cost and would allow the structure to remain operational while any inspections and minor repairs were made.

Notwithstanding the success of the experiment, it is considered there is still room for improvement. The energy dissipation devices needed to be replaced following each event. These devices were mounted externally to facilitate quick replacement between tests. However, such an arrangement may be too obtrusive in a real building. Alternative mounting locations should be examined or reusable internal devices should be considered. Furthermore, there remains constructability issues related to this system that have not been addressed by this study, particularly regarding displacement compatibility between the frame and floor slabs. The joint detailing configuration tested has proved that it is possible to reduce material and labor costs without sacrificing performance of the system. The unbonded prestress system was designed to yield at a reduced cross section bolt bar at large displacements. The aim was to provide additional energy dissipation in extreme events. However, as this would require the system to be re-stressed, it may be prudent to design the system to yield at very large (>8%) drifts and instead provide more robust supplemental energy dissipation devices.

Although the angled post-tensioning profile provided redundancy and easy access to jacking points, it significantly increased the complexity of the column joint. This congestion ended up governing the size of the column. By utilizing a straight tendon profile, where bars are coupled at the cast in-situ end, this congestion problem may be eliminated.

The cast in-situ closure-pour that used high strength fiber-reinforced concrete performed better than the normal strength concrete joint. Approximately half as much cracking occurred, and those cracks which did form did not open or propagate as significantly as the other joint. For example, the crack formed by the diagonal compression strut in both beams opened to only 1/3 the width in the west (high strength concrete) beam as in the east beam. Including such detailing strategies, possibly by casting all beam ends in-situ with high strength concrete, would lead to a reduction in damage at the joint. It is considered that such an in-situ joint located at least at one end is desirable to avoid potentially large on-site construction misalignment issues and allow the beams to be cast to reasonable tolerance.

CONCLUSIONS

Bi-directional quasi-earthquake displacement testing was performed on an 80% scale concrete frame sub-assemblage designed for damage avoidance. Critical earthquake records were selected probabilistically to represent multiple performance levels and a multi-level seismic performance assessment was conducted. Based on this dual experimental-computational study, the following conclusions are drawn:

1. Three performance objectives were met: (i) with high confidence it can be stated the structure will remain operational following a design level earthquake; (ii) with moderate confidence the structure will be repairable following a very rare earthquake; and (iii) with high confidence the structure will not collapse following a very rare earthquake.

2. A cast in-situ closure pour at one beam end helps alleviate construction tolerance issues and ensures the face of the beam is aligned properly with the column. The performance of this joint was satisfactory.
3. Steel energy dissipaters had to be replaced after each test. High efficiency, reusable energy dissipaters would further eliminate repair costs.
4. A hand method for predicting the subassembly response using rigid body kinematics was shown to provide reasonable agreement with results from testing. The results, however, showed more energy dissipation than predicted by the hand method. This was attributed to unpredictable friction forces from the bent tendons.

REFERENCES

1. Housner, G. W. 1963. The behavior of Inverted Pendulum Structure During Earthquake. *Bulletin of the Seismological Society of America*; **53**(2):403-417.
2. Aslam, M. Goddon, W.G. and Scalise, D.T. 1980. Earthquake Rocking Response of Rigid Blocks, *Journal of Structural Engineering*, *ASCE*; **106**(2):377-392.
3. Stone, W.C. Cheok, G.S. and Stanton, J.F. 1995. Performance of hybrid moment-resisting precast beam-column concrete connection subjected to cyclic loading. *ACI Journal*; **91**(2).
4. Priestley, M.J.N. Sritharan, S. Conley, J.R. Pampanin, S. 1999. Preliminary Results and Conclusions from the PRESSS Five-Story Precast Concrete Test Building. *PCI Journal*; **44**(6):42-67
5. Mander, J.B. and Cheng, C.T. 1997. Seismic Resistance of Bridge Piers Based on Damage Avoidance Design. *Technical Report* NCEER-97-0014 (*National Centre of Earthquake Engineering Research*), Department of Civil, Structural and Environmental Engineering, State University of New York at Buffalo, New York, USA

6. Solberg, K. Mashiko, N. Dhakal, R.P. Mander, J.B. 2006. Performance of a damage-protected highway bridge pier subjected to bidirectional earthquake attack. *Proceedings of the 19th Australasian Conference on the Mechanics of Structures and Materials* (ACMSM 18). Christchurch, NZ, pp. 437-442.

7. Standards New Zealand. 2006. NZS 3101: Part 1: 1995: Concrete Structures Standard, *Standards New Zealand*, Wellington.

8. Arnold, D.M. 2004. Development and Experimental Testing Of a Seismic Damage Avoidance Designed Beam to Column Connection Utilizing Draped Unbonded Post-Tensioning *ME Thesis,* Department of Civil Engineering, University of Canterbury, Christchurch, New Zealand.

9. Davies, M.N. 2004. Seismic Damage Avoidance Design of Beam-Column Joints using Unbonded Post-Tensioning: Theory, Experiments and Design Example. *ME Thesis,* Department of Civil Engineering, University of Canterbury, Christchurch, New Zealand.

10. Li, L. 2006, Further Experiments on Damage Avoidance design of Beam-to-column joints. *ME Thesis*, Dept. of Civil Engineering, University of Canterbury, Christchurch New Zealand

11. Amaris, A. Pampanin, S. Palermo, A. 2006. Uni and bi-directional quasi-static tests on alternative hybrid precast beam column joint subassemblies. *Proceedings of the 2006 New Zealand Society for Earthquake Engineering* (NZSEE) *Conference*. Napier, New Zealand, Paper #24.

12. Dutta, A. Mander, J.B. Kokorina, T. 1999. Retrofit for control and reparability of damage. *Earthquake Spectra*; **15**(4):657-679.

13. Dhakal, R.P. Mander, J.B. Mashiko, N. 2006. Identification of Critical Earthquakes for Seismic Performance Assessment of Structures, *Earthquake Engineering and Structural Dynamics;* **35**(8):989-1008.

14. Bull, D. and Brunsdon, D. 1998. Examples of Concrete Structural Design to New Zealand Standards 3101. *Cement and Concrete Association*, New Zealand.

15. Pampanin, S. Priestley, M.J.N Sritharan, S. 2001. Analytical Modeling of the Seismic Behavior of Precast Concrete Frames Designed with Ductile Connections. *Journal of Earthquake Engineering*; **5**(3): 329-367.

16. Carr A.J. 2006. Ruaumoko3D: Inelastic Dynamic Computer Program. *Computer Program Library,* Department of Civil Engineering, University of Canterbury, Christchurch, New Zealand.

17. Bradley, B.A. Dhakal, R.P. Mander, J.B. 2006 Dependency of current Incremental Dynamic Analysis to source mechanisms of selected records. *19th Biennial Conference on the Mechanics of Structures and Materials*; Christchurch, NZ. (in press).

18. Vamvatsikos D. and Cornell C.A., 2002, Incremental Dynamic Analysis. *Earthquake Engineering and Structural Dynamics*; **31**:491–514.

TABLES AND FIGURES

List of Tables:

List of Figures:

Table 1– Earthquake records selected for QED testing

Event	Year	Level	Max drift (%)[1]
N-Palos Verdes[2]	1992	90% DBE	2.1
N-Tabos	1974	50% MCE	2.8
M-Loma Prieta	1989	90% MCE	4.7

[1]Absolute value of radial peak interstory drift considering drifts in X and Y directions

[2]Simulated ground motion

N: Near source records; M: Medium source records (from SAC strong motion database)

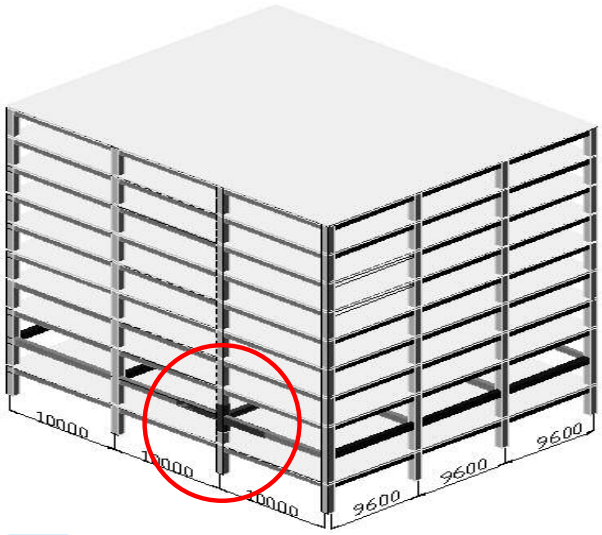

Fig. 1 – The prototype structure showing the location of the subassembly.

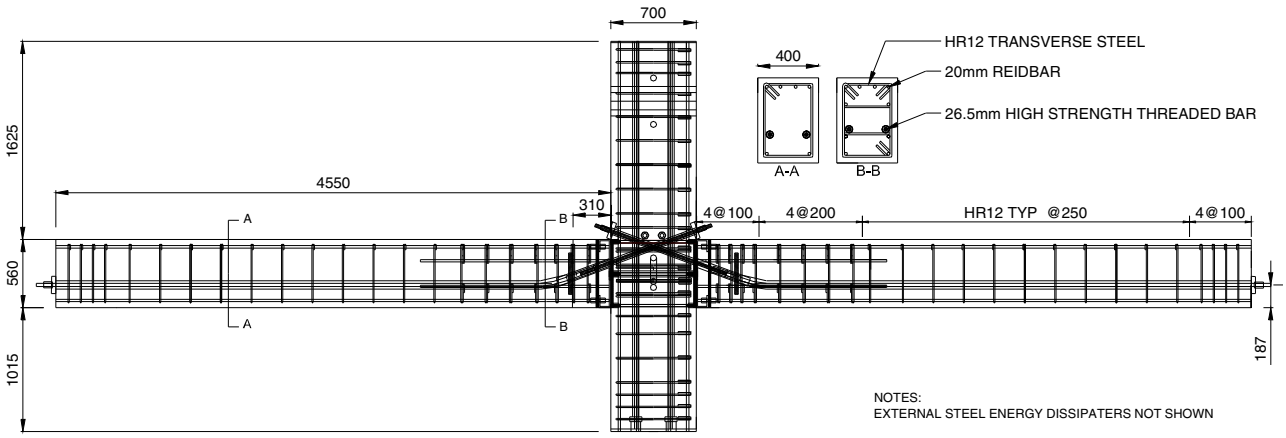

(a) Elevation view of the seismic beams and column.

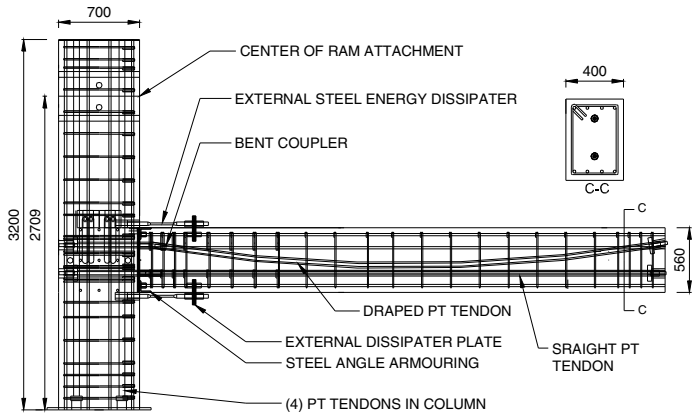

(b) Elevation view of the gravity beam and column.

Fig. 2 – Details of beams and column.

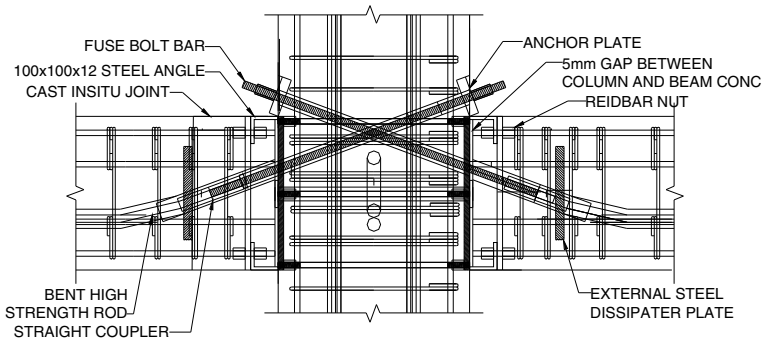

Fig. 3 – Detail of the column to seismic beams connections.

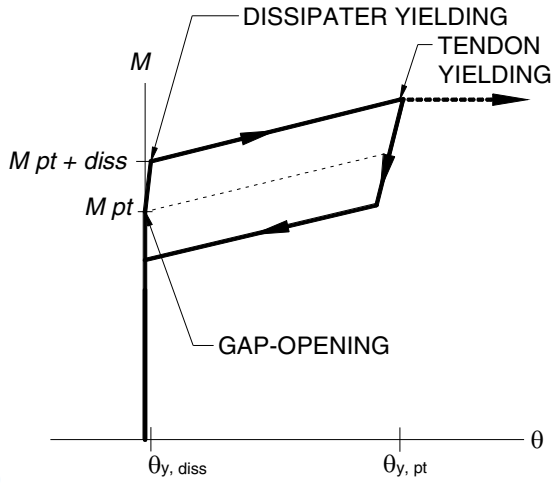

(a) Theoretical moment-rotation response of the rocking connection.

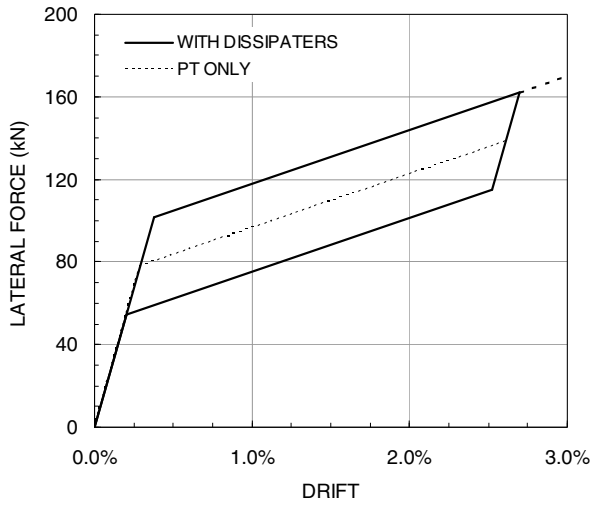

(b) Theoretical force-displacement response of the subassembly in the EW direction.

Fig. 4 – Theoretical prediction of the specimen's response.

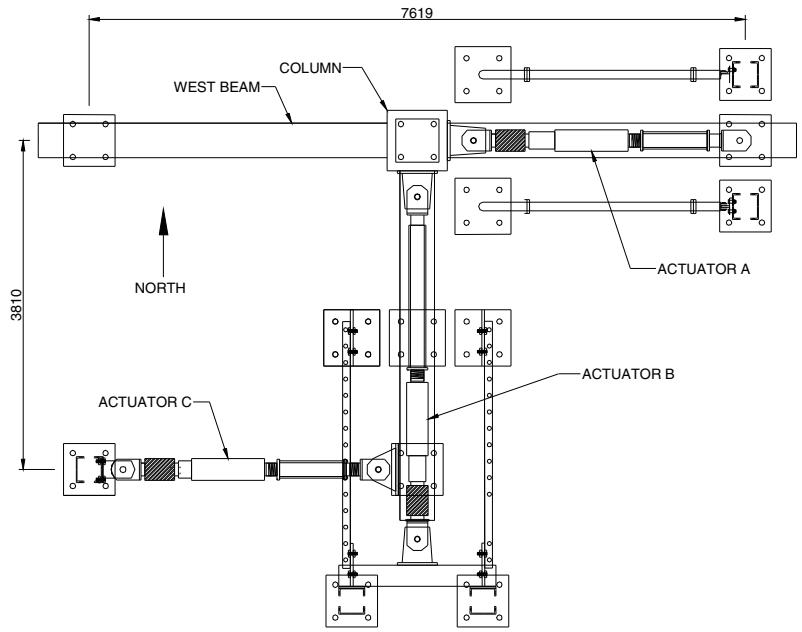

(a) Plan view of the test set-up.

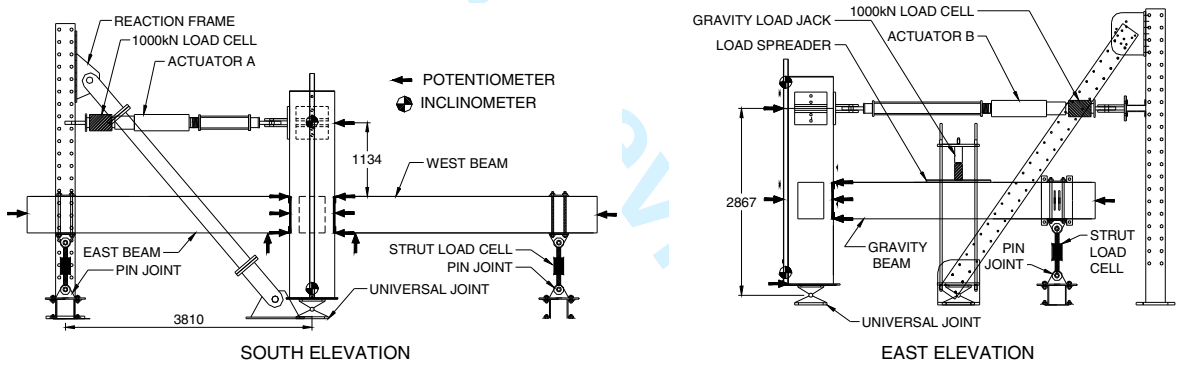

(b) Elevation of the test set-up.

(c) Photograph of the specimen in the test setup.

Fig. 5 – Test setup: specimen in the testing apparatus.

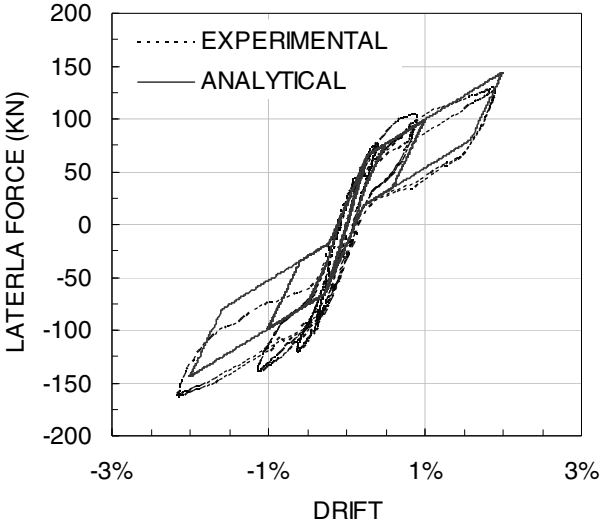

Fig. 6 – Experimental and analytical lateral force vs. drift response.

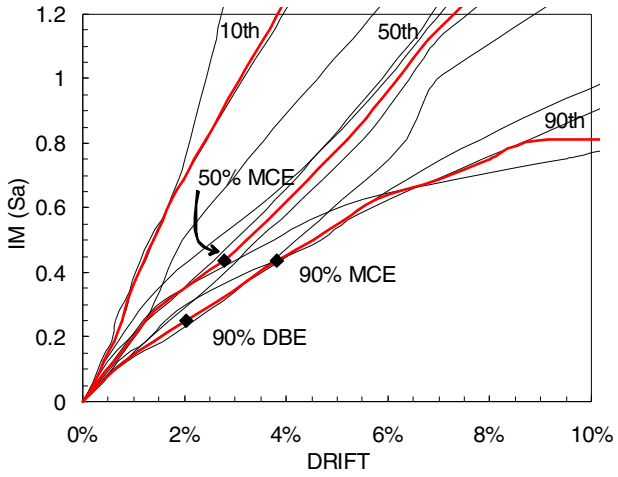

Fig. 7 – Earthquake record selection for the MSPA using IDA.

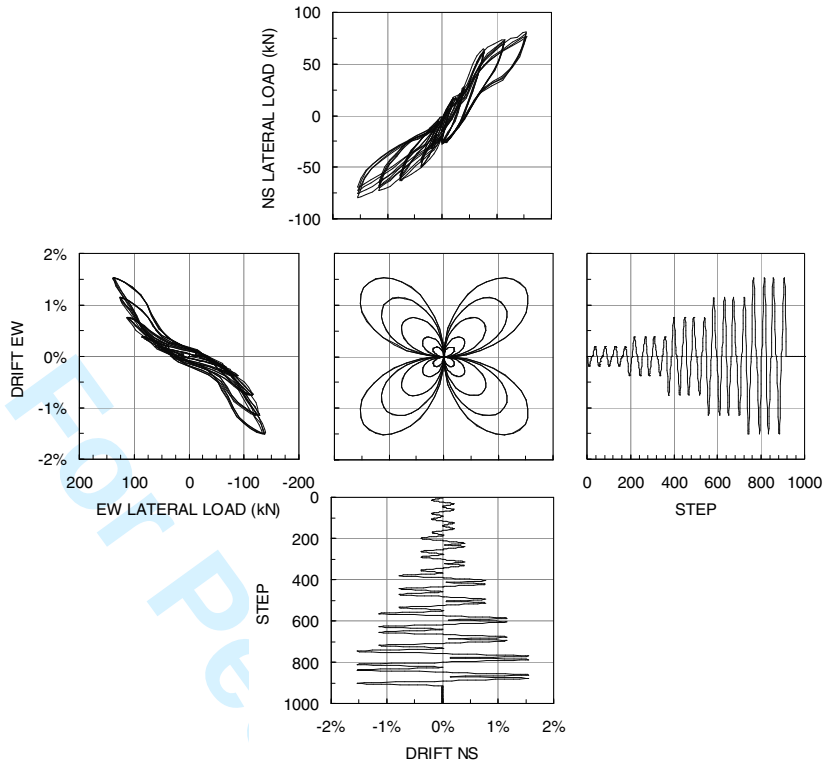

Fig. 8 – Force-displacement response from bi-directional "clover leaf" test.

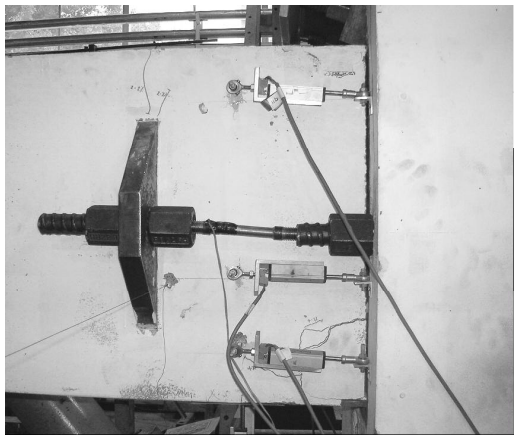

Fig. 9 – Photograph of the east seismic beam after the bi-directional quasi-static test to 2% drift.

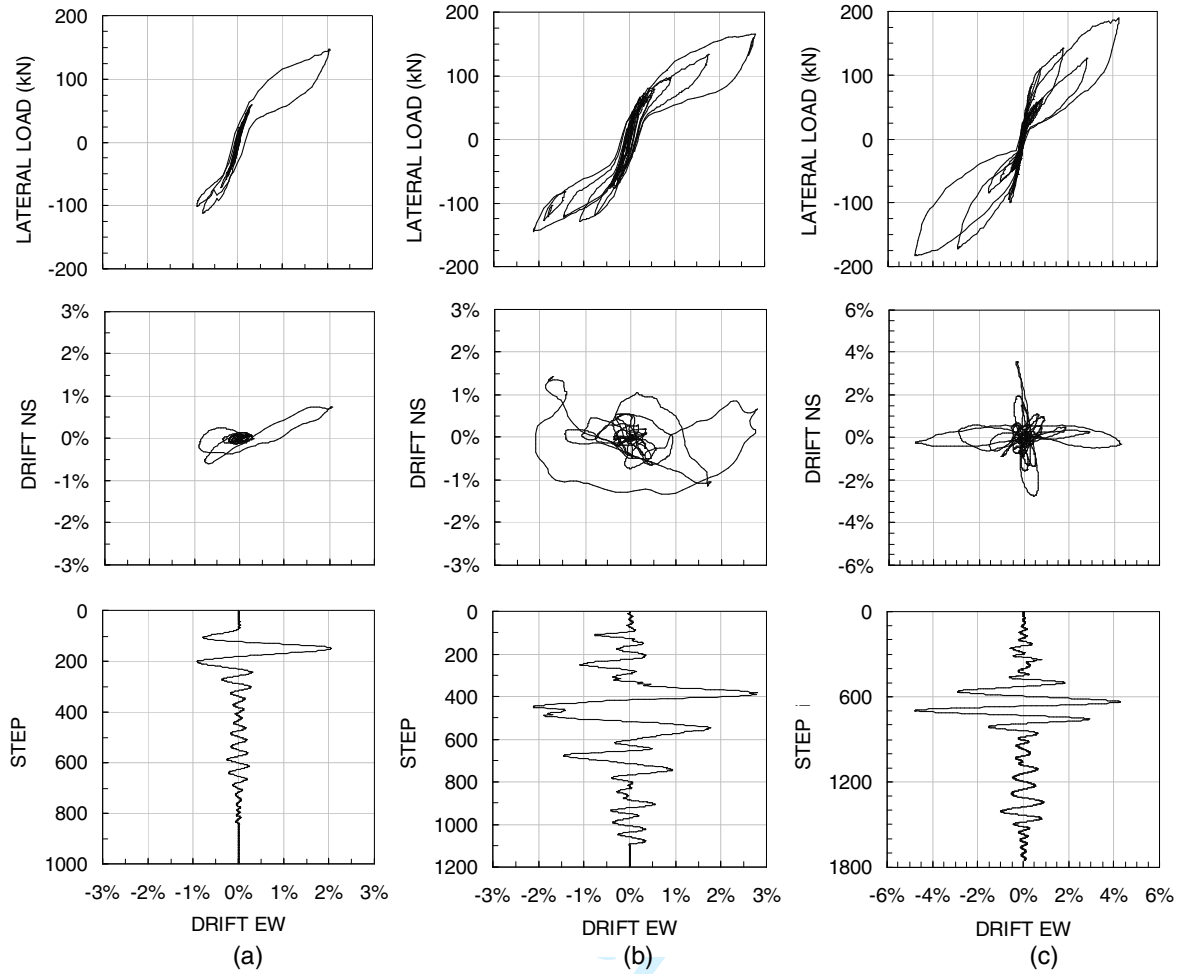

Fig. 10 – QED test results for the seismic beam (EW direction) for: (a) the 90% DBE; (b) the 50% MCE; and (c) the 90% MCE.

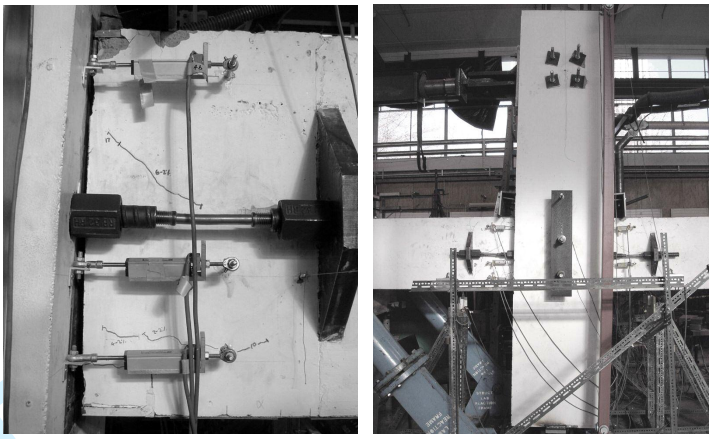

Fig. 11 – Photograph of the specimen during the 90% MCE test: (a) the west seismic beam joint at 4% drift; and (b) the specimen looking south at the maximum drift of 4%.

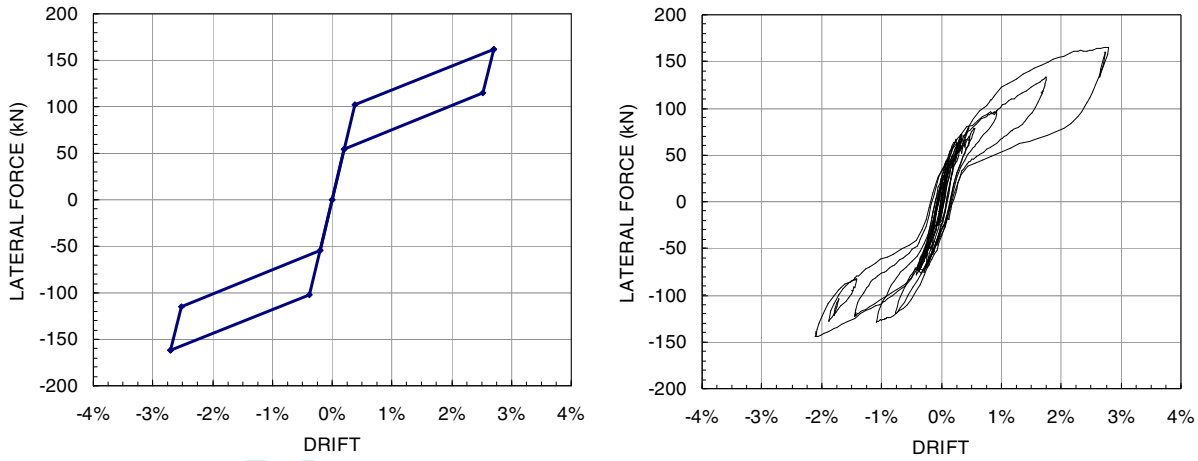

Fig. 12 – Comparison between: (a) the hand method; and (b) the experimental data for the 50th percentile MCE test.